

Critical Temperature Enhancement of Topological Superconductors: A Dynamical Mean Field Study

Yuki Nagai,¹ Shintaro Hoshino,² and Yukihiro Ota^{1,*}

¹*CCSE, Japan Atomic Energy Agency, 178-4-4, Wakashiba, Kashiwa, Chiba, 277-0871, Japan*

²*Department of Basic Science, The University of Tokyo, Meguro, Tokyo, 153-8902, Japan*

(Dated: June 20, 2016)

We show that a critical temperature T_c for spin-singlet two-dimensional superconductivity is enhanced by a cooperation between the Zeeman magnetic field and the Rashba spin-orbit coupling, where a superconductivity becomes topologically non-trivial below T_c . The dynamical mean field theory (DMFT) with the segment-based hybridization-expansion continuous-time quantum Monte Carlo impurity solver (ct-HYB) is used for accurately evaluating a critical temperature, without any Fermion sign problem. A strong-coupling approach shows that spin-flip driven local pair hopping leads to part of this enhancement, especially effects of the magnetic field. We propose physical settings suitable for verifying the present calculations, one-atom-layer system on Si(111) and ionic-liquid based electric double-layer transistors (EDLTs).

PACS numbers: 74.20.Rp, 74.25.-q, 74.25.Dw

Interesting materials properties are produced by the interplay between different internal degrees of freedom, such as spin and orbital, leading to the design of devices with useful characteristics [1, 2]. Manipulating spins in position or momentum space allows us to address exotic order in low-temperature physics. The application of Zeeman magnetic fields induces a spin imbalance in a system. Spin-orbit couplings (SOC) create a spin rotation depending on electron's motion. These effects lead to notable many-body ground states, such as the Fulde-Ferrel-Larkin-Ovchinnikov states [3–5], pair-density wave [6], and topological superfluidity/superconductivity [7–9].

The quest for high- T_c topological superconductors is a compelling issue in materials science. To reveal a way of enhancing T_c with keeping topological characters enables us to not only study topological order in a wide range of temperatures but also increase the feasibility of implementing topological quantum computing. Superconducting topological insulator $\text{Cu}_x\text{Bi}_2\text{Se}_3$ shows superconductivity at $T_c \sim 3.8\text{ K}$ [10], and is a candidate for bulk topological superconductors [10, 11]. Interestingly, its critical temperature is two orders of magnitude larger than a theoretical estimation with electron-phonon couplings [12]. Therefore, using a concrete theoretical method beyond the weak-coupling mean-field theory, clarifying the relevance of the key features of this compounds to T_c would lead to a clue of designing useful topological materials.

The presence of strong SOC is one of the crucial characters in $\text{Cu}_x\text{Bi}_2\text{Se}_3$, since the quasiparticle wavefunction has a strong momentum dependence due to the SOC so that the bulk state has a nontrivial topology[11]. This feature is common with other topological superconducting systems, such as ultra-cold atomic

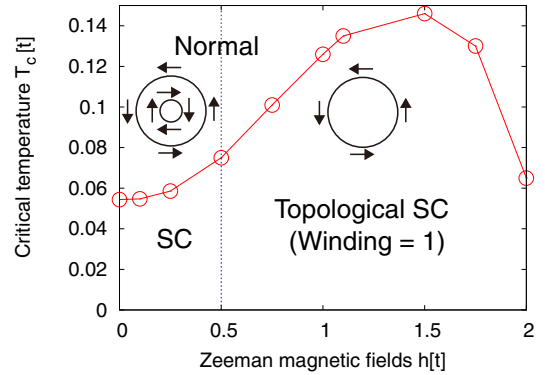


FIG. 1. (Color online) Zeeman-magnetic-field dependence of a critical temperature, with the attractive on-site coupling $U = -3t$, the spin-orbit coupling $\alpha = 1t$, the filling $\nu = 1/8$. The dash-dotted line shows that in a non-interacting case ($U = 0$) a winding number on the Fermi surfaces changes.

gases and artificial semiconductor-superconductor hetero structures [13]. Thus, it is interesting how spin degrees of freedom contribute to the critical temperature of topological superconductors.

An attractive idea of producing topological superconductors is to use 2D s -wave superconductors with spin manipulations [14]. Mean-field calculations predict that spin-singlet Cooper pairs have unconventional and topological characters in the presence of Rashba SOC and Zeeman magnetic fields [14–16]. This setting is suitable for assessing the connection between SOC and T_c , from two points of view. First, an intrinsic pair breaking (Pauli depairing) effect is involved, owing to the presence of Zeeman magnetic fields. Thus, one may understand how the contributions from SOC overcome the Pauli depairing effects. Second, a topologically non-trivial s -wave superconducting state is produced by an on-site attractive density-density interaction [14]. It indicates that an

* Present address: Research Organization for Information Science and Technology (RIST), 1-5-2 Minatojima-minamimachi, Kobe, 650-0047, Japan

arbitrary range of interaction strength can be systematically studied by a reliable theoretical method, the dynamical mean field theory (DMFT) [17] combined with a numerically exact continuous-time quantum Monte Carlo method [18, 19]. Utilizing this theoretical approach, one can take all kinds of local Feynman diagrams.

In this paper, we show that a 2D attractive Hubbard model with Rashba SOC possesses T_c enhancement even though the Zeeman magnetic field is applied. To treat an arbitrary strength of on-site U , we adopt the DMFT combined with a numerically exact continuous-time quantum Monte Carlo method. We point out that this approach accurately estimates T_c even in the present spin-active many-body system since a symmetric property of the many-body Hamiltonian in spin and k -space ensures the absent of the Fermion negative sign problem [19]. Our main results are shown in Fig. 1 and Fig. 2. The critical temperature on a certain filling changes with a non-monotonic manner, varying the magnitude of the Zeeman field and the Rashba SOC. A cooperation between the Zeeman field and SOC is a key of the T_c enhancement. A strong-coupling approach shows that the part of the enhancement (i.e. the magnetic field dependence) is explained by the local pair hopping [20], due to a spin-flip process. The rest of the enhancement (i.e., the SOC dependence) is still elusive. We speculate that the enhancement is related to a change of a winding number on the normal-electron Fermi surfaces. Moreover, we propose physical settings suitable for verifying the present calculations, one-atom-layer TI-Pb on Si(111) [21] and ionic-liquid based electric double-layer transistors (EDLTs) [22].

The single-orbital attractive Hubbard Hamiltonian with the Rashba SOC and the Zeeman magnetic field on 2D square lattice is [13, 14]

$$\mathcal{H} = \sum_{\mathbf{k}\sigma\sigma'} \hat{h}_0^{\sigma\sigma'}(\mathbf{k}) c_{\mathbf{k}\sigma}^\dagger c_{\mathbf{k}\sigma'} + U \sum_i n_{i\uparrow} n_{i\downarrow}, \quad (1)$$

where $\hat{h}_0(\mathbf{k}) = -\mu - 2t(\cos k_x + \cos k_y) + \alpha\mathcal{L}(\mathbf{k}) - h\hat{\sigma}_3$ and $n_{i\sigma} = c_{i\sigma}^\dagger c_{i\sigma}$ ($\sigma = \uparrow, \downarrow$). The hopping parameter, t is positive, whereas the coupling constant of the on-site interaction, U is negative. Throughout this paper, we use the unit system with $\hbar = k_B = 1$. The unit of energy is t . The electron annihilation (creation) operator with spin σ is $c_{i\sigma}$ ($c_{i\sigma}^\dagger$) on spatial site i . In the momentum representation they are $c_{\mathbf{k}\sigma}$ and $c_{\mathbf{k}\sigma}^\dagger$. The symbol $\hat{\sigma}_j$ is the j th component of the 2×2 Pauli matrices ($j = 1, 2, 3$). The Rashba SOC term is described by $\alpha\mathcal{L}(\mathbf{k}) = \alpha(\hat{\sigma}_1 \sin k_y - \hat{\sigma}_2 \sin k_x)$, with positive α . The strength of the Zeeman magnetic field is h . In our calculations, the chemical potential, μ is tuned, with fixed filling, ν .

Let us summarize the topological properties of a superconducting state in this model within the weak-coupling Bardeen-Cooper-Schrieffer (BCS) theory [14]. The topological number is the Thouless-Kohmoto-Nightingale-Nijs invariant [23, 24] on a 2D torus in the momentum

space. According to this invariant, the criteria of topological superconductivity are derived by Sato *et al.* (Table I in Ref. [14]). We focus on the case just below T_c ; the amplitude of the superconducting order parameter vanishes (i.e. $|\Delta| \rightarrow 0+$). Then, we find that the criteria in Ref. [14] are regarded as the changes of a winding number on the Fermi surfaces, where the winding number is defined as xy -plane spin rotation on the Fermi surfaces. Note that this characterization requires only the knowledge on the normal-state Fermi surfaces. The occurrence of a topological superconducting state just below T_c is associated with a non-zero winding number on the Fermi surfaces. Hence, although in this paper we only consider the normal states just above T_c , we can obtain a connection of normal-state instability with topological superconductivity.

We show our calculation method. To calculate one- and two-particle Green's functions, we utilize the DMFT with the segment-based hybridization-expansion continuous-time quantum Monte Carlo impurity solver (ct-HYB) [18, 25, 26]. The segment-based algorithm is the fastest update method of ct-HYB solvers, and is applicable to our system if (i) the interaction terms of the Hamiltonian conserve spin and (ii) in the effective Anderson impurity model the one-body local Hamiltonian does so. The first condition is satisfied since the system has only density-density interaction. Let us consider the second one. The one-body local Hamiltonian matrix, \hat{H}_f , is related to $\hat{h}_0(\mathbf{k})$ via [27]

$$\hat{H}_f = \sum_{\mathbf{k}} \hat{h}_0(\mathbf{k}) = -\mu - h\hat{\sigma}_3. \quad (2)$$

Since \hat{H}_f is diagonal in the spin space, the second condition is fulfilled. Moreover, we point out that there is no Fermion sign problem when self energy is diagonal in the spin space [19]. Since \mathcal{H} is invariant under the transformation $c_{\mathbf{k}\sigma} \rightarrow \sum_{\sigma'} (\hat{\sigma}_3)_{\sigma\sigma'} c_{-\mathbf{k}\sigma'}$, we find that the off-diagonal elements of self energy in the spin space are zero in the present system [28]. Accordingly, the evaluation of T_c is accurately performed by the DMFT with ct-HYB. In this paper, the effective impurity problem is solved by an open-source program package, *iQist* [29].

The main target in our calculations is the pair susceptibility with respect to a spin-singlet s -wave state at temperature T [30],

$$\chi = \frac{1}{N} \int_0^{1/T} \langle \mathcal{O}(\tau) \mathcal{O}^\dagger \rangle d\tau = T \sum_{nn'} \chi_{\uparrow\downarrow\uparrow\uparrow}(i\omega_n, i\omega_{n'}; 0), \quad (3)$$

with $\mathcal{O} = \sum_i c_{i\uparrow}^\dagger c_{i\downarrow}^\dagger$. The total number of lattice sites is N . The fermionic Matsubara frequency is $\omega_n = \pi T(2n + 1)$, with $n \in \mathbb{Z}$. Here, $\chi_{abcd}(i\omega_n, i\omega_{n'}; 0)$ is a two-particle lattice Green's function with a zero Bosonic Matsubara frequency. A divergence in χ (or equivalently a sign change in $1/\chi$) indicates a possible transition into a superconducting phase. In the effective im-

purity model one- and two- particle local Green's functions, $G_{ab}^{\text{loc}}(i\omega_n)$ and $\chi_{abcd}^{\text{loc}}(i\omega_n, i\omega_{n'}; 0)$ respectively, are calculated by the Gardenia component of the *iQist* package. One-particle Green's function in the original lattice model is $\hat{G}(\mathbf{k}, i\omega_n) \equiv [i\omega_n - \hat{h}_0(\mathbf{k}) - \hat{\Sigma}(i\omega_n)]^{-1}$, with self energy $\hat{\Sigma}(i\omega_n)$. Two-particle lattice Green's functions are obtained by simultaneously solving two Bethe-Salpeter equations with a common vertex function $\underline{\Gamma}$ [30, 31],

$$\underline{\chi}^{\text{loc}} = \underline{\tilde{\chi}}^{\text{loc},0} + \underline{\chi}^{\text{loc},0} \underline{\Gamma} \underline{\chi}^{\text{loc}}, \quad (4a)$$

$$\underline{\chi} = \underline{\tilde{\chi}}^0 + \underline{\chi}^0 \underline{\Gamma} \underline{\chi}. \quad (4b)$$

The double underline indicates that an object is a matrix on a vector space including two spin indices and the Matsubara frequency; $\chi_{abcd}(i\omega_n, i\omega_{n'})$ is embedded into $(\underline{\chi})_{ll'}$ with $l = (a, b, n)$ and $l' = (d, c, n')$, for example. We take all the processes of the DMFT framework, regardless of spin conservation or not. In the Bethe-Salpeter equations the matrix objects with superscript 0 contain bare two-particle Green's functions produced by one-particle Green's functions. In the effective impurity model, we have $\chi_{abcd}^{\text{loc},0}(i\omega_n, i\omega_{n'}) = \chi_{dacb}^{\text{loc},gg}(i\omega_n)\delta_{n,n'}$ and $\tilde{\chi}_{abcd}^{\text{loc},0}(i\omega_n, i\omega_{n'}) = \chi_{abcd}^{\text{loc},0}(i\omega_n, i\omega_{n'}) - \chi_{cadb}^{\text{loc},gg}(i\omega_n)\delta_{n,-n'-1}$, with $\chi_{abcd}^{\text{loc},gg}(i\omega_n) = G_{ab}^{\text{loc}}(i\omega_n)G_{cd}^{\text{loc}}(-i\omega_n)$. In a similar manner we define bare two-particle Green's functions in the lattice model; all local one-particle Green's functions are replaced with lattice one-particle Green's functions, and $\chi_{abcd}^{gg}(i\omega_n)$ is defined as $\chi_{abcd}^{gg}(i\omega_n) = \sum_{\mathbf{k}} G_{ab}(\mathbf{k}, i\omega_n)G_{cd}(-\mathbf{k}, -i\omega_n)$. In the calculation of the two-particle Green's functions, the \mathbf{k} -mesh size and the n -mesh size are 192×192 and 64, respectively. The numerical calculations on $\underline{\chi}$ are performed by an equation not explicitly including $\underline{\Gamma}$: $\underline{\chi} = \underline{\chi}^{\text{loc}}(\underline{1} - \underline{A})^{-1}\underline{B}$ with $\underline{A} \equiv ([\underline{\chi}^{\text{loc},0}]^{-1} - [\underline{\chi}^0]^{-1})\underline{\chi}^{\text{loc}} + \underline{1} - \underline{B}^{\text{loc}}$, $\underline{B} \equiv [\underline{\chi}^0]^{-1}\tilde{\chi}^0$ and $\underline{B}^{\text{loc}} \equiv [\underline{\chi}^{\text{loc},0}]^{-1}\tilde{\chi}^{\text{loc},0}$ (in detail, see Ref. [32]).

Figure 1 shows T_c with respect to the change of the Zeeman magnetic field when $\alpha = t$, $U = -3t$, and $\nu = 1/8$. The critical temperature increases with increasing h , and takes a peak around $h = 1.5t$. Then, the decrease of T_c occurs in a stronger magnetic field; this reduction corresponds to the Pauli depairing effect. We mention that the weak-coupling mean-field calculations indicate the complete suppression of T_c even in the weak magnetic field $h = 1t$ [See, e.g., Fig. 2(a) at $\alpha = 1t$]. We note that a weak-coupling approach in the presence of spatial phase fluctuations [33, 35] predicts the decrease of T_c with increasing Zeeman magnetic fields. We infer from Fig. 1 a relation between the T_c enhancement and the change of the winding number on the Fermi surfaces from 0 (conventional, non-topological, *s*-wave) to 1 (topological *s*-wave). To study this point more closely, we consider a different way of changing the winding number. We focus on a region of parameter sets in which the

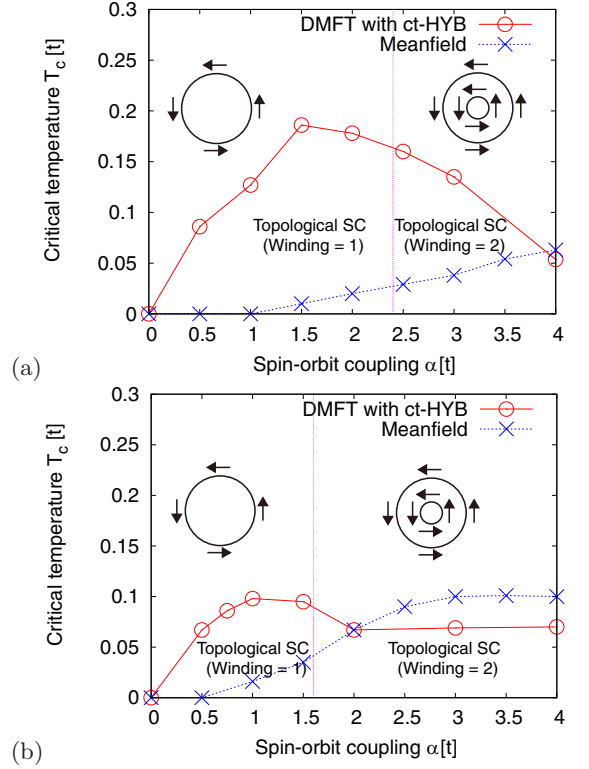


FIG. 2. (Color online) Spin-orbit coupling dependence of a critical temperature, with (a) Zeeman magnetic field, $h = t$ and filling, $\nu = 1/8$ and (b) $h = 0.5t$ and $\nu = 1/16$. The attractive on-site coupling, $U = -3t$, is common. Each vertical dash-dotted line has the same meaning as that in Fig. 1.

winding number transits from 1 to 2 increasing α with fixed ν and h . Figure 2 shows the behaviors of T_c in the DMFT calculations (red circle), as well as the results obtained by the weak-coupling mean-field calculations (blue cross). We find in the DMFT calculations that the behavior of T_c is non-monotonic as α . In contrast, the weak-coupling mean-field critical temperature monotonically grows up as α since the in-plane Rashba SOC may suppress the Pauli depairing effect induced by the Zeeman magnetic field along *z*-axis [34]. In the DMFT calculations, an optimal value of α in the enhancement of T_c locates at the region of the winding number to be 1. Thus, our calculations suggest that the parameter region in which the winding number is 1 be suitable for realizing a topological superconducting state at a high temperature. We stress that these results occur at different parameter sets, as shown in Figs. 2(a) and (b). It is important to note that calculating a topological invariant in interacting systems is desirable for finding the genuine topological transition point. The renormalized Zeeman magnetic field and the chemical potential due to the self-energy at the zero-energy [36] would shift the lines of winding-number changes in Figs. 1 and 2.

Now, we derive a strong-coupling-limit formula of T_c , to get the picture on the enhancement of T_c with respect

to the changes of α and h . In a strong-coupling limit $|U| \rightarrow \infty$, the model can be rewritten as a pseudospin ($S = 1/2$) quantum Heisenberg model, whose Hamiltonian is given by $\mathcal{H}_{\text{eff}} = \sum_{\langle ij \rangle} [-J(S_i^x S_j^x + S_i^y S_j^y) + JS_i^z S_j^z] - H \sum_i S_i^z$, where $\sum_{\langle ij \rangle}$ considers nearest-neighbors only and the pseudospin up and down states are doubly-occupied and unoccupied local states, respectively. The effective coupling constant and the pseudo spin field are $J(t, \alpha, h, U) \equiv 4t^2/|U| + |U|\alpha^2/(|U|^2 - 4h^2)$ and $H = -2\mu + U$, respectively. The mean-field analysis in this effective Hamiltonian gives the critical temperature. Thus, we obtain the expression of T_c ,

$$T_c(\alpha, h) = \frac{(1 - 2\nu)J(t, \alpha, h, U)}{\tanh^{-1}(1 - 2\nu)}. \quad (5)$$

We show that part of the enhancement (h -dependence of T_c) is explained by local pair hopping [20] in terms of the strong coupling approach. We find that, even in the half filling case ($\nu = 1/2$), the critical temperature enhances with increasing h , as shown in Fig. 3(a). A key of the enhancement of T_c is depicted in Fig. 3(b); a pair on the i th site can hop into the $i + 1$ th site via a virtual spin-flip process coming from non-vanishing α of second-order perturbation (lower diagram on the middle panel). A strong Zeeman magnetic field splits the energy levels between the spin-flip (lower diagram) and spin-conserved (upper diagram) processes; the presence of the Zeeman field tends to increase the rate of the spin-flip process. Therefore, this spin-flip-driven local pair hopping is responsible for the T_c enhancement under nonzero h , although most of our DMFT calculations are outside strong-coupling regime since the energy of the singly-occupied state is smaller than the energies of the doubly-occupied and empty states. In Ref. [32], we also show that the spin-flip processes are important for the T_c enhancement in the DMFT calculations.

The local-pair-hopping scenario, however, does not fully explain the behavior of T_c . Under the fixed Zeeman magnetic field, the dependence of T_c on α in the strong-coupling formula is quite different from the DMFT calculations, as shown in Fig. 2; the critical temperature in the DMFT calculations is *not* a monotonic increase function of α , even though the Pauli depairing effect could be suppressed for large α . We can find that the DMFT calculations with $U = -7t$ are consistent with the strong-coupling formula; T_c monotonically increases within our calculations in $0 \leq \alpha \leq 4t$. Thus, explaining the α -dependence of T_c in an intermediate range of on-site U would require for a different scenario. It is an interesting future issue of unveiling the remaining origin of T_c enhancement. We speculate that focusing on the change of the winding number might give us an insight on this elusive issue.

Now, we propose two physical systems available for testing our theoretical calculations. The first setup is to apply Zeeman magnetic fields to one-atom-layer TI-Pb compounds on Si(111). Matetskiy *et al.* [21] observed the

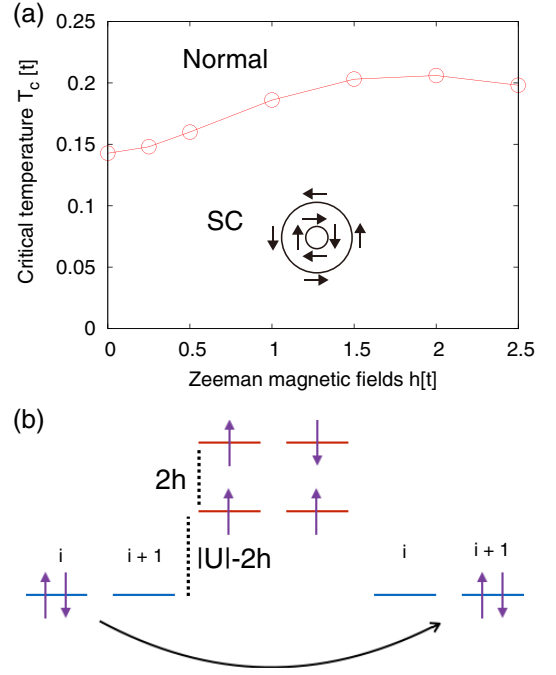


FIG. 3. (Color online) (a) Zeeman magnetic field dependence of a critical temperature at half filling ($\nu = 1/2$). Other settings are equal to those in Fig. 1. (b) Schematic diagram of pair hopping from the i th to the $(i + 1)$ th sites via either spin-flip (lower panel) or spin-conserved (upper panel) processes.

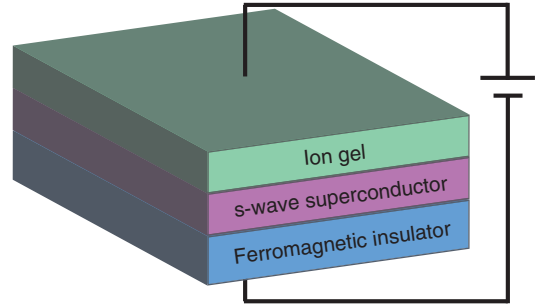


FIG. 4. (Color online) Schematic figure of ionic-liquid based electric double-layer transistors (EDLTs).

occurrence of giant Rashba effects in this setting without the Zeeman field. The second setup is to use EDLT with a layered structure built up by an s -wave superconductor and a ferromagnetic insulator, as shown in Fig. 4. The idea of fabricating related systems is shown in Fig. 2(a) of Ref. [22]. Tuning electric fields allows us to control electron's filling and the strength of SOC. This EDLT setup would be a plausible system to design 2D topological superconductors.

Finally, we discuss a link of our calculations with $\text{Cu}_x\text{Bi}_2\text{Se}_3$, from the viewpoint of T_c enhancement. Although the present system is quite different from

$\text{Cu}_x\text{Bi}_2\text{Se}_3$, we have an interesting correspondence between the two systems. One of the authors (Y.N.) found in the calculations of impurity effects [37] that the presence of orbital imbalance leads to similar effects to those induced by a spin imbalance, even though an external magnetic field is absent. In the present system a strong Zeeman magnetic field induces the coherent hopping of a localized pair via a spin-flip process, leading of the increase of T_c . Hence, in $\text{Cu}_x\text{Bi}_2\text{Se}_3$, a large orbital imbalance might cause an orbital-flip process contributing to the enhancement of T_c . The DMFT study in the model of $\text{Cu}_x\text{Bi}_2\text{Se}_3$ is our important future issue.

In summary, we showed that a 2D attractive Hubbard model with Rashba SOC and a Zeeman magnetic field possesses T_c enhancement, by using the DMFT combined with the numerically exact ct-HYB solver without any Fermion sign problem. With the use of a strong-coupling

approximation, part of the enhancement (i.e. the magnetic field dependence) was explained by the scenario of a local pair hopping induced by a spin-flip process. The rest of the enhancement (i.e. the SOC dependence) is still in an open issue. We speculated that the enhancement is related to a change of a winding number of the normal-electron Fermi surfaces. Moreover, we proposed that EDLTs are good stages for designing topological superconductivity. Finally, we discussed a high T_c in $\text{Cu}_x\text{Bi}_2\text{Se}_3$ with the use of the result in our two-dimensional system.

Y. N. thanks Y. Saito for helpful comments on the EDLTs. The calculations were performed by the supercomputing system SGI ICE X at the Japan Atomic Energy Agency. This study was partially supported by JSPS KAKENHI Grants No. 26800197 and No. 15K00178.

-
- [1] I. Žutić, J. Fabian, and S. Das Sarma, Spintronics: Fundamentals and applications, *Rev. Mod. Phys.* **76**, 323 (2004).
 - [2] M. Z. Hasan and C. L. Kane, Colloquium: Topological insulators, *Rev. Mod. Phys.* **82**, 3045 (2010).
 - [3] P. Fulde and R. A. Ferrell, Superconductivity in a Strong Spin-Exchange Field, *Phys. Rev.* **135**, A550 (1964).
 - [4] A. I. Larkin and Y. N. Ovchinnikov, Nonuniform state of superconductors, *Zh. Eksp. Teor. Fiz.* **47**, 1136 (1964) [*Sov. Phys. JETP* **20** 762 (1965)].
 - [5] Y. Yanase, Angular Fulde-Ferrell-Larkin-Ovchinnikov state in cold fermion gases in a toroidal trap, *Phys. Rev. B* **80**, 220510 (2009).
 - [6] T. Yoshida, M. Sigrist, and Y. Yanase, Pair-density wave states through spin-orbit coupling in multilayer superconductors, *Phys. Rev. B* **86**, 134514 (2012).
 - [7] A. Y. Kitaev, Unpaired Majorana fermions in quantum wires, *Phys. Usp.* **44**, 131 (2001).
 - [8] C. Nayak, S.H. Simon, A. Stern, M. Freedman, and S. D. Sarma, Non-Abelian anyons and topological quantum computation, *Rev. Mod. Phys.* **80**, 1083 (2008).
 - [9] J. Alicea, New directions in the pursuit of Majorana fermions in solid state systems, *Rep. Prog. Phys.* **75**, 076501 (2012).
 - [10] S. Sasaki, M. Kriener, K. Sagawa, K. Yada, Y. Tanaka, M. Sato and Y. Ando, Topological Superconductivity in $\text{Cu}_x\text{Bi}_2\text{Se}_3$, *Phys. Rev. Lett.* **107**, 217001 (2011).
 - [11] L. Fu and E. Berg, Odd-Parity Topological Superconductors: Theory and Application to $\text{Cu}_x\text{Bi}_2\text{Se}_3$, *Phys. Rev. Lett.* **105**, 097001 (2010).
 - [12] X.-L. Zhang and W.-M. Liu, Electron-Phonon Coupling and its implication for the superconducting topological insulators, *Sci. Rep.* **5**, 8964 (2015).
 - [13] J. D. Sau, R. M. Lutchyn, S. Tewari, and S. D. Sarma, Generic New Platform for Topological Quantum Computation Using Semiconductor Heterostructures, *Phys. Rev. Lett.* **104**, 040502 (2010).
 - [14] M. Sato, Y. Takahashi, and S. Fujimoto, Non-Abelian topological orders and Majorana fermions in spin-singlet superconductors, *Phys. Rev. B* **82**, 134521 (2010).
 - [15] A. Shitade and Y. Nagai, Orbital angular momentum in a nonchiral topological superconductor, *Phys. Rev. B* **92**, 024502 (2015).
 - [16] Y. Nagai, Y. Ota, and M. Machida, Impurity effects in a two-dimensional topological superconductor: A link of T_c -robustness with a topological number, *J. Phys. Soc. Jpn.* **83**, 094722 (2014).
 - [17] A. Georges, G. Kotliar, W. Krauth, and M.J. Rozenberg, Dynamical mean-field theory of strongly correlated fermion systems and the limit of infinite dimensions, *Rev. Mod. Phys.* **68**, 13 (1996).
 - [18] P. Werner and A. J. Mills, Hybridization expansion impurity solver: General formulation and application to Kondo lattice and two-orbital models, *Phys. Rev. B* **74**, 155107 (2006).
 - [19] E. Gull, A. J. Millis, A. I. Lichtenstein, A. N. Rubtsov, M. Troyer, and P. Werner, Continuous-time Monte Carlo methods for quantum impurity models, *Rev. Mod. Phys.* **83**, 349 (2011).
 - [20] R. Micnas, J. Ranninger, and S. Robaszkiewicz, Superconductivity in narrow-band systems with local nonretarded attractive interactions, *Rev. Mod. Phys.* **62**, 113 (1990).
 - [21] A.V. Matetskiy, S. Ichinokura, L.V. Bondarenko, A.Y. Tupchaya, D.V. Gruznev, A.V. Zotov, A.A. Saranin, R. Hobara, A. Takayama, and S. Hasegawa, Two-Dimensional Superconductor with a Giant Rashba Effect: One-Atom-Layer Tl-Pb Compound on Si(111), *Phys. Rev. Lett.* **115**, 147003 (2015).
 - [22] L. J. Li, E. C.T. O'Farrell, K. P. Loh, G. Eda, B. Özyilmaz, and A. H. Castro Neto, Controlling many-body states by the electric-field effect in a two-dimensional material, *Nature* (2015) doi:10.1038/nature16175.
 - [23] D. J. Thouless, M. Kohmoto, M. P. Nightingale, and M. den Nijs, Quantized Hall Conductance in a Two-Dimensional Periodic Potential, *Phys. Rev. Lett.* **49**, 405 (1982).
 - [24] M. Kohmoto, Topological invariant and the quantization of the Hall conductance, *Ann. Phys.* **160**, 343 (1985).
 - [25] K. Haule, Quantum Monte Carlo impurity solver for cluster dynamical mean-field theory and electronic structure

- calculations with adjustable cluster base, Phys. Rev. B **75**, 155113 (2007).
- [26] P. Werner, A. Comanac, L. Medici, M. Troyer, and A. J. Millis, Continuous-Time Solver for Quantum Impurity Models, Phys. Rev. Lett. **97**, 076405 (2006).
- [27] As $|\omega_n| \rightarrow \infty$, local Green's functions in the original and effective impurity models are $\hat{G}^{\text{loc}}(i\omega_n) \sim 1/(i\omega_n) + (\sum_{\mathbf{k}} \hat{h}_0(\mathbf{k}) + \hat{\Sigma}_0)/(i\omega_n)^2$ and $\hat{G}_f(i\omega_n) \sim 1/(i\omega_n) + (\hat{H}_f + \hat{\Sigma}_0)/(i\omega_n)^2$, respectively, with the zero-th order self-energy $\hat{\Sigma}_0$. Thus, the self-consistent condition in the DMFT, $\hat{G}^{\text{loc}}(i\omega_n) = \hat{G}_f(i\omega_n)$, leads to Eq. (2).
- [28] Local Green's function is $\hat{G}^{\text{loc}}(i\omega_n) = a\hat{1} + b\hat{\sigma}_3$ when the self-energy is diagonal in spin space. The hybridization function in the ct-HYB becomes diagonal in this case.
- [29] Li Huang, Yilin Wang, Zi Yang Meng, Liang Du, Philipp Werner and Xi Dai, iQIST: An open source continuous-time quantum Monte Carlo impurity solver toolkit, Comp. Phys. Comm. **195**, 140 (2015).
- [30] S. Hoshino and P. Werner, P Superconductivity from emerging magnetic moments, Phys. Rev. Lett. **115**, 247001 (2015).
- [31] J.K. Freericks, M. Jarrell and D.J. Scalapino, Holstein model in infinite dimensions, Phys. Rev. B **48**, 6302 (1993).
- [32] See Supplemental materials for the detail arguments on our DMFT calculations.
- [33] Y. Xu and C. Zhang, Berezinskii-Kosterlitz-Thouless Phase Transition in 2D Spin-Orbit-Coupled Fulde-Ferrell Superfluids, Phys. Rev. Lett. **114**, 110401 (2015).
- [34] Solving the mean-field BCS linearized gap equations, we have $T_c \sim T_c^0 \exp \left[\frac{1}{|U|} \left[\frac{1}{N^0} - \frac{1}{N(\alpha, h)} \right] \right]$ if $\alpha \gg h$. Here, T_c^0 and N^0 are a critical temperature and a density of states at the Fermi energy for $h = 0$ and $\alpha = 0$, respectively. The weak-coupling formula indicates that T_c is subjected to the density of states on the Fermi surfaces $N(\alpha, h)$, which monotonically increases as α when ν is fixed.
- [35] J. P. A. Devreese, J. Tempere, and C. A. R. Melo, Effects of Spin-Orbit Coupling on the Berezinskii-Kosterlitz-Thouless Transition and the Vortex-Antivortex Structure in Two-Dimensional Fermi Gases, Phys. Rev. Lett. **113**, 165304 (2014).
- [36] Z. Wang and S.-C. Zhang, Simplified Topological Invariants for Interacting Insulators, Phys. Rev. X **2**, 031008 (2012).
- [37] Y. Nagai, Robust superconductivity with nodes in the superconducting topological insulator $\text{Cu}_x\text{Bi}_2\text{Se}_3$: Zeeman orbital field and nonmagnetic impurities, Phys. Rev. B **91**, 060502(R) 2015.

Supplemental materials

S1. Two Bethe-Salpeter equations

This section closely shows a heart of our formulation in a system with spin-orbital couplings. The pair susceptibility with respect to a spin-singlet s -wave state χ is Eq. (3) in the main text. A divergence in χ (or equivalently a sign change in $1/\chi$) indicates a possible transition into a superconducting phase. This quantity is obtained by simultaneously solving two Bethe-Salpeter equations, one of which is formulated in an effective impurity model, while another of which does in the original lattice model. The Bethe-Salpeter equation for the effective impurity model is expressed as

$$\begin{aligned} \chi_{aa'a'a}^{\text{loc}}(i\omega_n, i\omega_{n'}) &= \left(\chi_{aaa'a'}^{\text{loc},0}(i\omega_n)\delta(\omega_n - \omega_{n'}) - \chi_{a'aaa'}^{\text{loc},0}(i\omega_n)\delta(\omega_n + \omega_{n'})\delta_{a'a} \right) \\ &+ \sum_{n_1, n_2} \left[\chi_{aaa'a'}^{\text{loc},0}(i\omega_n)\delta(\omega_n - \omega_{n_1}) \right] \Gamma_{a'aaa'}(i\omega_{n_1}, i\omega_{n_2}) \chi_{aa'a'a}^{\text{loc}}(i\omega_{n_2}, i\omega_{n'}). \end{aligned} \quad (\text{S1})$$

The subscripts (a , a' , and so on) represent spin indices, equal to those in the main text. Here, we assume the spin-diagonal one-body local Hamiltonian [See Eq. (2) in the main text] and the density-density interaction. The bare local two-particle Green's function $\chi_{abcd}^{\text{loc},0}(i\omega_n)$ is defined by

$$\chi_{abcd}^{\text{loc},0}(i\omega_n) = G_{ab}^{\text{loc}}(i\omega_n)G_{cd}^{\text{loc}}(-i\omega_n), \quad (\text{S2})$$

with $\hat{G}^{\text{loc}}(i\omega_n) \equiv \sum_{\mathbf{k}} \hat{G}(\mathbf{k}, i\omega_n) = \sum_{\mathbf{k}} [i\omega_n - \hat{h}_0(\mathbf{k}) - \hat{\Sigma}(i\omega_n)]^{-1}$ calculated by an impurity solver. Note that Eq. (S1) can be solved with fixed indices (a , a'), separately. Thus, one can obtain $\chi_{\uparrow\uparrow\uparrow\uparrow}^{\text{loc}}(i\omega_n, i\omega_{n'})$, $\chi_{\uparrow\downarrow\downarrow\uparrow}^{\text{loc}}(i\omega_n, i\omega_{n'})$, $\chi_{\downarrow\uparrow\uparrow\downarrow}^{\text{loc}}(i\omega_n, i\omega_{n'})$, and $\chi_{\downarrow\downarrow\downarrow\downarrow}^{\text{loc}}(i\omega_n, i\omega_{n'})$, separately, with the use of the impurity solver for the system where the spin is conserved. On the other hand, the Bethe-Salpeter equation for the original lattice model is expressed as

$$\begin{aligned} \chi_{aa'a'a}(i\omega_n, i\omega_{n'}) &= (\chi_{aaa'a'}^0(i\omega_n)\delta(\omega_n - \omega_{n'}) - \chi_{a'aaa'}^0(i\omega_n)\delta(\omega_n + \omega_{n'})) \\ &+ \sum_{n_1, n_2} \sum_{a_1, a_2, a_3, a_4} [\chi_{a_2aa_1a'}^0(i\omega_n)\delta(\omega_n - \omega_{n_1})] \Gamma_{a_1a_2a_3a_4}(i\omega_{n_1}, i\omega_{n_2}) \chi_{a_3a_4a'a}(i\omega_{n_2}, i\omega_{n'}). \end{aligned} \quad (\text{S3})$$

Here, the vertex $\Gamma_{a_1a_2a_3a_4}(i\omega_{n_1}, i\omega_{n_2})$ is equal to that in the local Bethe-Salpeter equation (S1). The bare original lattice two-particle Green's function $\chi_{abcd}^0(i\omega_n)$ is defined by

$$\chi_{abcd}^0(i\omega_n) = \sum_{\mathbf{k}} G_{ab}(\mathbf{k}, i\omega_n)G_{cd}(-\mathbf{k}, -i\omega_n). \quad (\text{S4})$$

To solve two Bethe-Salpeter equations simultaneously, we introduce an expression $\underline{\chi}$ on a vector space including two spin indices and the Matsubara frequency. $\chi_{abcd}(i\omega_n, i\omega_{n'})$ is embedded into $(\underline{\chi})_{ll'}$ with $l = (a, b, n)$ and $l' = (d, c, n')$, for example. The numerical calculations on $\underline{\chi}$ are performed by an equation not explicitly including $\underline{\Gamma}$:

$$\underline{\chi} = \underline{\chi}^{\text{loc}}(\underline{1} - \underline{A})^{-1}\underline{B}, \quad (\text{S5})$$

with $\underline{A} \equiv ([\underline{\chi}^{\text{loc},0}]^{-1} - [\underline{\chi}^0]^{-1})\underline{\chi}^{\text{loc}} + \underline{1} - \underline{B}^{\text{loc}}$, $\underline{B} \equiv [\underline{\chi}^0]^{-1}\tilde{\chi}^0$ and $\underline{B}^{\text{loc}} \equiv [\underline{\chi}^{\text{loc},0}]^{-1}\tilde{\chi}^{\text{loc},0}$. The above expression is numerically stable, since the inverse matrices $[\underline{\chi}^{\text{loc},0}]^{-1}$ and $[\underline{\chi}^0]^{-1}$ are diagonal in the Matsubara space.

S2. Comparison with full and spin-conserved processes

In this section, we show that the spin-flip processes are important for the T_c -enhancement in the main text. The full spin-singlet pairing susceptibility $\chi_{\uparrow\downarrow\downarrow\uparrow}(i\omega_n, i\omega_{n'})$ includes both spin-conserved and spin-flip processes. The Rashba spin-orbit coupling in Eq. (1) in the main text induces spin-flipping processes. If the two-particle Green's function is constructed by the spin-conserved processes only, the Bethe-Salpeter equation (S3) in the original lattice system becomes

$$\chi_{\uparrow\downarrow\downarrow\uparrow}(i\omega_n, i\omega_{n'}) = \chi_{\uparrow\uparrow\downarrow\downarrow}^0(i\omega_n)\delta(\omega_n - \omega_{n'}) + \sum_{n_1, n_2} [\chi_{\uparrow\uparrow\downarrow\downarrow}^0(i\omega_n)\delta(\omega_n - \omega_{n_1})] \Gamma_{\downarrow\uparrow\uparrow\downarrow}(i\omega_{n_1}, i\omega_{n_2}) \chi_{\uparrow\downarrow\downarrow\uparrow}(i\omega_{n_2}, i\omega_{n'}). \quad (\text{S6})$$

We show the divergences of χ in $1/\chi$ in Fig. S1. We consider both cases with full and spin-conserved processes. Figure S1(a) shows that the critical temperature T_c with full processes is larger than that with spin-conserved processes in the system with $h = 0$ and $\alpha = 1$. Figure S1(b) shows that the results by solving both equations are same in the system without the spin orbit coupling. There is no critical temperature, since the Pauli depairing effect is so strong that the Cooper pairs are destroyed. Figures S1(c) and (d) show that the spin-flip processes are important to induce the superconducting phase. The spin-conserved processes can not overcome the Pauli depairing effect so that the critical temperature is zero.

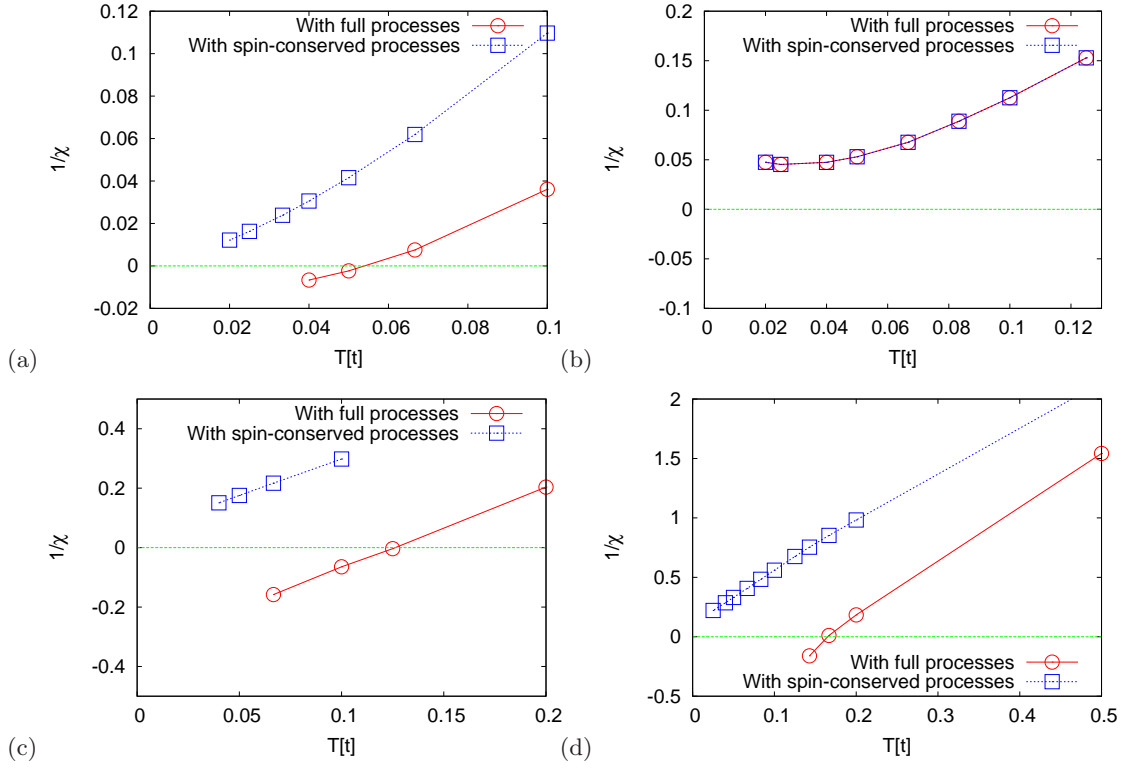


FIG. S1. (Color online) Sign changes of $1/\chi$ with (a) $h = 0$ and $\alpha = 1$, (b) $h = 1$ and $\alpha = 0$, (c) $h = 1$ and $\alpha = 1$, and (d) $h = 1$ and $\alpha = 2$. The red circles denote the result by solving Eq. (S3) and the blue squares denote the result by solving Eq. (S6). The filling $\nu = 1/8$ and the attractive on-site coupling $U = -3t$.